The Danish SAR system: design and initial tests

Madsen, Søren Nørvang; Christensen, Erik Lintz; Skou, Niels; Dall, Jørgen

Published in:
I E E E Transactions on Geoscience and Remote Sensing

Link to article, DOI:
10.1109/36.79432

Publication date:
1991

Document Version
Publisher's PDF, also known as Version of record

The Danish SAR System: Design and Initial Tests

Søren Nørvang Madsen, *Member, IEEE*, Erik Lintz Christensen, Niels Skou, *Member, IEEE*, and Jørgen Dall

***Abstract*—In January 1986 the design of a high-resolution airborne *C*-band Synthetic Aperture Radar (SAR) started at the Electromagnetics Institute of the Technical University of Denmark. The initial system test flights took place in November and December 1989. The purpose of this paper is to describe the design of the system, its implementation, and performance. The paper will show how digital technology has been utilized to realize a very flexible radar with variable resolution, swathwidth, and imaging geometry. The motion-compensation algorithms implemented to obtain the high resolution will be outlined, as well as the special features built into the system to ensure proper internal calibration. The data processing system, developed for the image generation and quality assurance, will be sketched, with special emphasis on the flexibility of the system. Sample images and a preliminary performance evaluation will be presented, demonstrating that the design goals have been met. Finally, the on-going system upgrades and the planned scientific utilization of the *C*-band SAR will be described.**

***Keywords*—High-resolution airborne SAR, SAR system design, SAR calibration.**

I. Introduction

THE principle of Synthetic Aperture Radar (SAR) was discovered nearly 40 years ago, and the first unclassified papers were published 20 years ago [1]. For many years SAR was mainly of military interest, primarily due to the fact that civilian applications could not justify the development of the costly SAR systems. Therefore the development of SAR's focused on military needs such as high resolution and long range. Today, the benefits of SAR for remote sensing is widely recognized and a number of SAR's have been built not only for research but also for operational applications such as sea-ice surveillance.

In the spring of 1986 the Electromagnetics Institute of the Technical University of Denmark initiated a project to develop a high-resolution airborne SAR. The project, sponsored by the Thomas B. Thriges Foundation, has also benefitted extensively by the aircraft support from the Royal Danish Air Force.

The KRAS (Coherent Radar and Advanced Signal processing) system which is described in this paper is a research radar which serves the dual purpose of being: (i) A testbed for coherent radar technology; and (ii) a facility for underflights in support of the European ERS-1 SAR satellite.

Since the study of advanced digital technology is an important part of the project, the radar is based on digital electronics to the highest possible degree. All units are controlled and monitored by the radar control computer. All signals are generated, recorded, and processed digitally. This approach has resulted in a very flexible radar which supports different mapping geometries, resolutions, swaths, and calibration modes.

Section II describes the design requirements, followed by the implementation details in Section III. Section IV outlines the motion compensation approach, and Section V focuses on the calibration features built into the system as well as some accuracy and stability measurements. The data processing system is discussed in Section VI. Section VII describes the first tests of the radar and the evaluation of the first results, and finally, Section VIII discusses ongoing activities and future plans.

II. KRAS Design Requirements

The system parameters corresponding to the present configuration are listed in Table I.

A. Frequency and Polarization

The system's frequency and polarization were determined to be suitable for underflight campaigns for the European ERS-1 SAR satellite [2], now scheduled for launch in early 1991. This fixed the frequency to 5.3 GHz and the polarization to *VV*.

B. Mapping, Modes, Geometry

The ERS-1 satellite SAR acquires data at steep angles of incidence ($23 \pm 3°$), necessitating operation at very high altitudes (since useful "simulation swath" at the relevant incidence angle interval is proportional to altitude). Accordingly, the design was optimized for operation at altitudes in the range 30 000 to 45 000 ft. The potential applications of the Danish SAR range widely from geophysical mapping, sea ice monitoring, and fishery inspection, all requiring wide swath and moderate resolution (i.e., 10 m), to cartographic mapping and reconnaissance, where high resolution is a primary concern. The wide range of applications requires incidence angles from 20° to 80°, leading to a requirement for a steerable antenna depression (tilt) angle.

Manuscript received September 27, 1990; revised January 10, 1991. This work was supported by the Thomas B. Thriges Foundation.

S. Nørvang Madsen is on leave from the Electromagnetics Institute of the Technical University of Denmark, Building 348, DK-2800 Lyngby, Denmark. He is presently working at the Jet Propulsion Laboratory, California Institute of Technology, 4800 Oak Grove Drive, Pasadena, CA 91109.

E. Lintz Christensen, N. Skou, and J. Dall are with the Electromagnetics Institute of the Technical University of Denmark, Building 348, DK-2800 Lyngby, Denmark.

IEEE Log Number 9143274.

0196-2892/91/0500-0417$01.00 © 1991 IEEE

TABLE I
KRAS SYSTEM PARAMETERS

Frequency	5.3 GHz
Transmitter peak power	2 kW
Receiver noise figure	2.5 dB
System loss (estimate)	3 dB
Pulse length	from 0.64 to 20 μs
Maximum bandwidth	100 MHz
Antenna gain	26.8 dB
azimuth 3-dB beamwidth	2.7°
elevation pattern width	30°
polarization	*VV*
Resolution	
range	variable 2, 4, 8 m
azimuth	variable 2, 4, 8 m
Slant-range swath (raw data)	variable 12, 24, 48 km
Maximum range	80 km

C. Resolution and Swath

The multipurpose emphasis mentioned above prescribed a requirement for a variety of resolutions (from 2 by 2 m) and variable swath widths. The nominal range of the system was set at 80 km and the maximum slant range swath width (after pulse-compression) ranges from 9 km (at 2-m resolution) to 48 km (at 8-m resolution). The swath is limited by the maximum number of complex range cells (8192). This also establishes the requirement for the elevation beamwidth of 30° to ensure a swath not constrained by the antenna characteristics (however, in the nadir-looking mode the swath is beam limited). A programmable data window off-set is also essential. Three typical mapping set-ups are shown in Fig. 1.

D. Sensitivity

The system sensitivity requirement is to map distributed targets with a characteristic backscatter coefficient of $\sigma^\circ = -30$ dB (m^2/m^2) at an incidence angle of $\theta = 65^\circ$ (altitude 12.5 km, slant range = 30 km) with a 10 dB SNR (−40 dB $NE\sigma^0$ = noise-equivalent-sigma-zero), which again corresponds to a point-target sensitivity of 10 dB SNR for a point target with $\sigma = 0.1$ m^2 at a range of 80 km. (A simple calculation based on the parameters in Table I, using 2-m resolution, 20 μs pulse length, and a PRF of 1 pulse per 0.1875 m gives $NE\sigma^0 = -42.5$ dB, and $\sigma = 0.043$ m^2.)

E. Calibration

System calibration was a primary consideration, although vaguely defined due to uncertainties regarding the (stability) performance of available components. The goal was set at ±1 dB absolute calibration, and extensive calibration features are part of the baseline system.

F. Aircraft and Installation

It was required that the radar should fit in a rather small (executive type) jet aircraft. The radar should support true ground speeds up to 580 kn (290 m/s) and operation up to 45 000 ft (13 720 m). Also, a requirement was that it could be mounted or dismounted in 2 h.

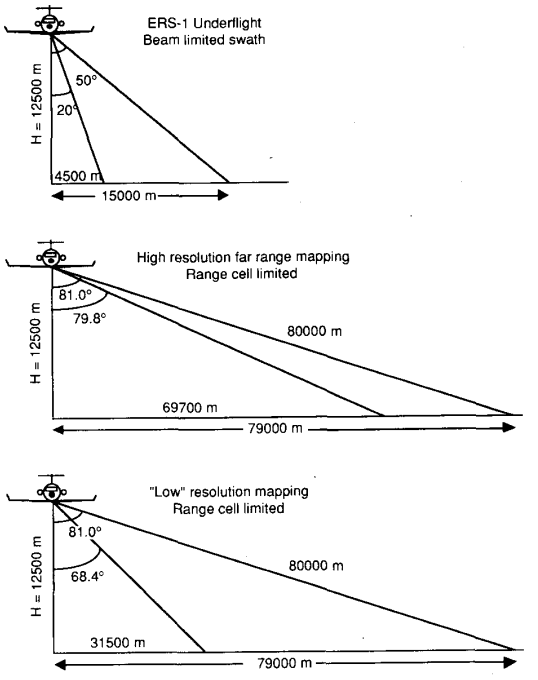

Fig. 1. Examples showing some possible mapping configurations for the KRAS SAR.

III. SYSTEM IMPLEMENTATION

A. Radar Electronics

The system is based on a conventional heterodyne approach (although a homodyne design was considered [3]) using a 300-MHz IF frequency and a 5-GHz RF local oscillator. All timing signals in the radar front-end are phase-locked to the IF frequency. The system block diagram is shown in Fig. 2.

The required flexibility with respect to resolution and swath is obtained by digital signal generation in the transmitter and digital preprocessing in the receiver. The transmitted waveform is generated by the control computer in-flight in accordance with the bandwidth, pulse duration, and coding type selected by the operator. From the control computer it is down-loaded in a fast buffer memory. This approach provides maximum flexibility and also allows predistortion of the signal, enabling corrections of system errors such as the lack of quadrature or balance in the modulator, transfer function errors, etc., resulting in improved range sidelobes. The price paid for this flexibility is that a large, fast buffer memory is required; 4096 complex code words are stored in the RAM buffer, supporting pulses of lengths up to 20.48 μs. The signal is read out to two DA converters running at a 200-MHz sampling rate, low-pass filtered with a cut-off frequency of 150 MHz, and then I/Q modulated to 300 MHz. The performance of the predistortion system is described in more detail by Netterstrøm, [4].

The I/Q modulator and the up-converter transforms the baseband signal into a 5.3-GHz RF signal (variable) that

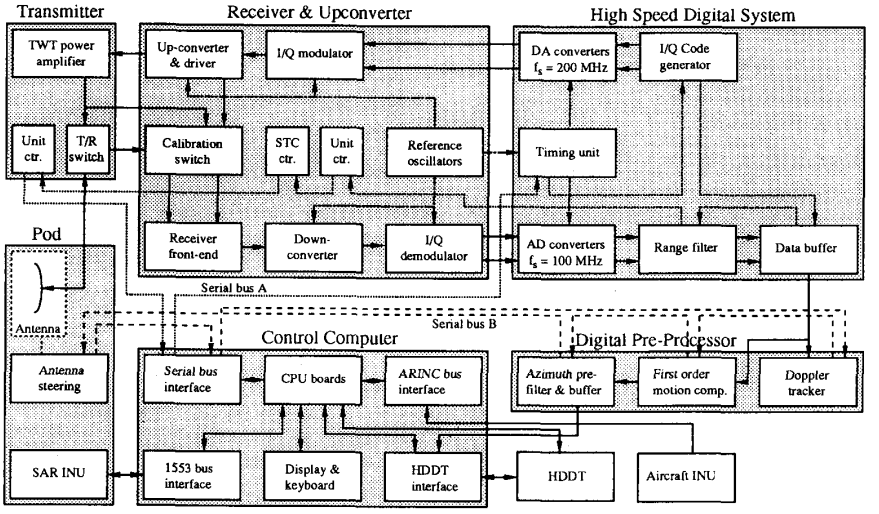

Fig. 2. Radar block diagram.

is amplified to +23 dBm by a solid-state driver, which is input to the traveling wave tube (TWT). As described later, both the driver and TWT signals are connected to the calibration system. The 2-kW output of the TWT is then routed to the antenna via a T/R switch. The received echoes are routed from the antenna, via the T/R switch to a low-noise amplifier (LNA) and a calibration switch module into the receiver. The dynamic range of the system is optimized by use of a variable attenuator (40 dB variation range) at the RF level. This attenuator is used both for constant gain setting and sensitivity time control (STC). The received signal is bandlimited at the IF and converted to baseband using a quadrature demodulator. The I and Q baseband signals are converted to digital signals by two 8-b, 100 MHz AD-converters [5].

B. Digital On-Line Preprocessing

The output of the AD-converters passes through a line of real-time modules labeled range filter, data buffer, MoComp 1, and azimuth prefilter, [6]. The range filters (I&Q) are 100-MHz, finite impulse response filters which can be programmed to low-pass filter and subsample the received signal. In the low-resolution modes, the SNR is improved by low-pass filtering the I and Q signals before they are subsampled. The range filter can subsample by factors of 1, 2, or 4, thereby reducing the data rate and widening the swath by the same factors. The range filter is followed by a buffer memory, which in its simplest modes, suits the purpose of converting the high data rate/low duty cycle to a lower data rate at a duty cycle of 80 to 95%. A first-order motion compensation (range-independent phase shifts) is applied by the Mocomp 1 module. It also down-converts the signal azimuth spectrum to zero Doppler offset and thereby preconditions the signal for the programmable azimuth prefilter, which low-pass filters and subsamples the signal in azimuth. The KRAS SAR operates at PRF's higher than needed to sample the signal properly and achieve the desired resolution. In combination with the azimuth prefiltering, the oversampling of the Doppler spectrum improves the SNR. The subsample factors are 1, 2, 4, 8, and 16. The azimuth prefilter is followed by another buffer memory implementing the data rate reduction/duty cycle increase that is enabled by the subsampling.

In addition to the active systems in the signal path, a Doppler estimation system based on the sign Doppler algorithm is included [7]. The system can be configured such that this board either precedes or follows Mocomp 1. The function of this subsystem is described in more detail in the section on motion compensation.

C. Antenna

The antenna is a 1.2-m-long, slotted, waveguide phased-array antenna with an elevation pattern resembling a modified cosec square pattern ($G(\psi) \sim \operatorname{cosec}^2\psi \sqrt{\cos\psi}$). The antenna consists of four separate panels to maximize the available bandwidth. For further details see [8].

To assist planning the system performance, a number of plots showing the received power as a function of altitude, antenna tilt angle, and ground range have been generated, and an example is shown in Fig. 3. The plots assume a constant backscatter coefficient, $\sigma^0 = -20$ dB (m^2/m^2), and are based on the measured antenna pattern, a 3-dB system loss, and a 20-μs transmitted pulse. The noise floor using a 100-MHz receive bandwidth is at -91.5 dBm. Due to signal oversampling (especially in azimuth), the SNR of the processed image is improved, as mentioned earlier.

D. Antenna Installation

The antenna is mounted in a modified fuel pod from a Draken fighter. The center part of the pod is replaced by a $\lambda/4$ matched A-sandwich radome (two layers of fiber-

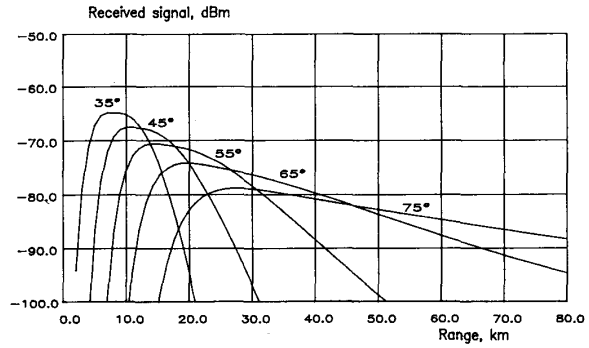

Fig. 3. Plot showing the return power from a $\sigma^\circ = -20$ dB target as a function of look angle for a flight altitude of 41 000 ft.

glass separated by a low density foam) which gives a reflection coefficient below -17 dB over the full range of incidence angles [9]. The attitude of the antenna is controlled by a 3 degree of freedom drive. The antenna is attached to the pod by a ball pivot. Three linear actuators control the antenna pointing, based on aircraft motion information from an INU (Inertial Navigation Unit) which is mounted in the pod next to the antenna to minimize lever-arm corrections [10].

The dimensions of the antenna and pod limit the antenna pitch, yaw, roll, and tilt/depression angles to: $\theta P = \pm 3.3°$; $\theta_Y = \pm 10°$; $\theta_R = \pm 5°$; and $\theta_D = 15°$–$55°$. For the Gulfstream G-3 aircraft this satisfies nearly all flight conditions.

E. Control Computer

The entire radar is controlled by a multiprocessor VME-bus-based control computer system, CC [11]. The operation of the SAR is assisted by "automap" software. Combining the great circle flight path (known from INU measurements) and the scene center entered by the operator, the automap software calculates the slant-range offset and the antenna depression angle. Likewise, it automatically starts and stops the mapping based on the aircraft position and scene size. The CC initializes all radar units and controls them automatically or by operator input. The operator communication can be via a menu-driven touch screen or by key board. It generates codes for the digital pulse generator and calculates STC tables as well as filter coefficients for the range filter and azimuth prefilter. The CC communicates with the radar INU and controls the PRF and the antenna pointing based on INU measurements. It combines INU and Doppler-tracker measurements and provides real-time motion compensation parameters. Also, it includes numerous BITE (Built-In Test Equipment) facilities and software to analyze acquired data.

F. Aircraft

The radar is presently installed on a Gulfstream G-3 aircraft (owned and operated by the Royal Danish Air Force). This provides a stable platform that operates at a nominal airspeed of 240 m/s. It is especially well suited for satellite underflights, since it can operate at high altitudes (up to 45 000 ft). The antenna installation was placed under the fuselage near the wings (see Fig. 4).

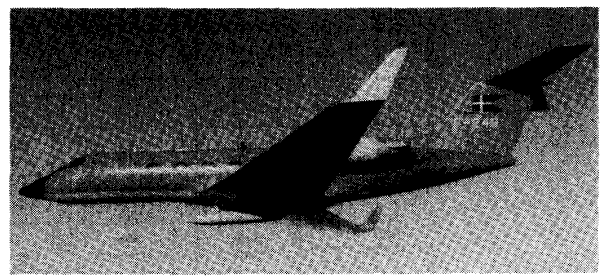

Fig. 4. Gulfstream G-3 with the SAR pod mounted below the fuselage.

IV. Motion Compensation

In general, formation of the synthetic aperture requires the radar to move along a smooth known trajectory, in the aircraft case a straight line. For aircraft high-resolution systems, such smooth uniform motion is not feasible and some type of motion compensation is essential. In this section, mocomp problems in general, and those specific to the KRAS SAR implementation will be outlined. The problem essentially is that the antenna does not follow the required straight displacement pattern. Additionally, it will exhibit a time-dependent pointing in response to the aircraft yaw, pitch, and roll.

The first problem is to measure where the radar is relative to the nominal aperture location. This is usually done by an INU, which uses gyros (mechanical or laser) to measure angles, and accelerometers to measure displacements. However, the practical problems in these measurements are significant. They include quantization errors, insufficient sampling frequencies, time delays on output, sensor drift, etc. These problems have been described in [12]. A second problem is to find the line-of-sight (LOS) vector from the radar to the target, since the slant-range displacement that needs to be determined is given by:

$$\Delta R = \vec{n}_{\mathrm{LOS}} \cdot \Delta \vec{r}_{\mathrm{ant}} = |\Delta \vec{r}_{\mathrm{ant}}| \cdot \cos(\theta_{\mathrm{ant}} - \theta_{\mathrm{LOS}}) \quad (1)$$

where according to Fig. 5, $\vec{n}_{\mathrm{LOS}}$ is a unit vector in the LOS direction, $\Delta \vec{r}_{\mathrm{ant}}$ is the antenna displacement vector, and θ_{ant}–θ_{LOS} is the angle between the LOS and radar displacement (angles are measured relative to vertical). The LOS angle is not known; only the slant range (R) and a platform altitude relative to average terrain are available. It is easily shown that an altitude error of Δh will give rise to an angle error $\Delta\theta$ given by:

$$\Delta\theta = \frac{\Delta h}{R \cdot \sin\theta_{\mathrm{LOS}}}. \quad (2)$$

It is seen that for satellite simulation underflights where the angle of incidence is small (20°–30°), it is extremely difficult to determine the LOS angle accurately. At 20° incidence angle and 12-km altitude, even a 50-m height

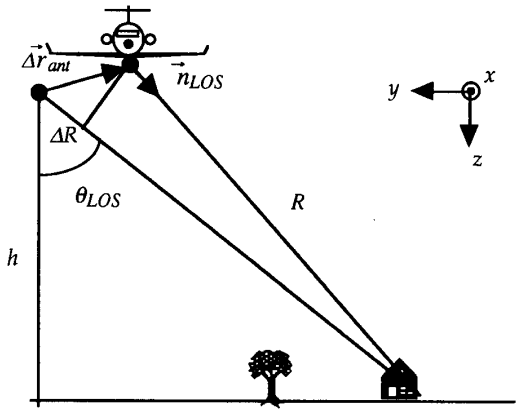

Fig. 5. The motion compensation geometry.

uncertainty will give 0.6° uncertainty on the LOS angle corresponding to a residual error of 1% on the motion-correction factor. (Obviously a stable platform is always preferable.)

The implementation of a computationally efficient system is also difficult. In principle, all received echoes should be range-compressed to obtain an accurate slant-range measurement before motion compensation. By performing the range compression after the azimuth prefiltering, the computational load, which is especially important in relation to a real-time implementation, is significantly reduced. As the azimuth prefilter is a Doppler low-pass filter equivalent to a short first-order beam forming, data should ideally be motion-compensated before the prefilter. Still, an analysis has shown that in the KRAS case, the apertures formed by the prefilter are so short that it is only required to phase-compensate the data before the prefilter, with a range-migration correction performed later. Secondly, it has been found that the signal will not be significantly attenuated (<0.3 dB) in the prefilter, even if the same phase correction is used for the entire range line. The processing algorithm is therefore:

1) Perform first-order motion compensation on the raw range line consisting of a common phase shift of the entire range line
2) Prefilter the data in azimuth (usually reducing the PRF by 4 or 8)
3) Range compress the data
4) Perform the second-order motion compensation, which is residual phase correction, and the range migration correction, both being functions of range (the already performed phase shift must be subtracted)
5) Continue the "standard processing."

A major problem is that INU velocities tends to drift with time. Since the antenna pointing is controlled by the INU, the drift results in a misorientation of the antenna relative to the synthetic array cross track. It also causes errors in the along-track velocity estimate, leading to focus problems. A Doppler tracker has been implemented to enable updates of the INU velocities. It provides a number of Doppler estimates as a function of slant range. Defining the flight direction as the x-axis, the z-axis pointing down, and y completing a right-hand coordinate system, it is found for the left-looking KRAS system (Fig. 5) that the Doppler shift is given by the cross-track velocities as:

$$f_D = \frac{2}{\lambda}(v_y \sin\theta_{\mathrm{LOS}} - v_z \cos\theta_{\mathrm{LOS}}). \tag{3}$$

The estimates cover 64 (or 128 programmable) range intervals from near to far range and therefore correspond to different angles of incidence. The observations can be modeled as:

$$\begin{pmatrix} f_{D1} \\ \vdots \\ f_{Dn} \end{pmatrix} = \frac{2}{\lambda}\begin{pmatrix} k_{11} & k_{12} \\ \vdots & \vdots \\ k_{n1} & k_{n2} \end{pmatrix}\begin{pmatrix} v_y \\ v_z \end{pmatrix} = \frac{2}{\lambda}\boldsymbol{k}\begin{pmatrix} v_y \\ v_z \end{pmatrix} \tag{4}$$

where $k_{i1} = \sin\theta_i$, and $k_{i2} = -\cos\theta_i$. It can be shown that the minimum square estimator for the transversal velocities is given by:

$$\begin{pmatrix} \hat{v}_y \\ \hat{v}_z \end{pmatrix} = \frac{\lambda}{2}(\boldsymbol{k}^T\boldsymbol{k})^{-1}\boldsymbol{k}^T\vec{f}_D \tag{5}$$

where $\boldsymbol{k}^T$ is the transposition of $\boldsymbol{k}$. In some mapping geometries the elevation angle interval is so narrow that the uncertainty on the cross-line-of-sight component is unacceptable. Therefore the actual implementation of the algorithm is slightly more complex using LOS/cross-LOS velocities instead of v_y and v_z so that only the LOS velocity estimates are used for up-dating the INU velocity biases in these cases.

The v_x velocity is the most critical parameter for long-range, high-resolution mapping. The tolerance on v_x corresponding to 45° quadratic phase error is:

$$\Delta v_x = \frac{v_x(\rho_a)^2}{\lambda R} = \frac{v_x}{2\mathrm{TB}_{\mathrm{azm}}} \tag{6}$$

where ρ_a is the azimuth resolution, and $\mathrm{TB}_{\mathrm{azm}}$ is the azimuth time bandwidth product. To achieve a 2-m resolution at 80-km range requires an accuracy of 0.2 m/s on the along-track velocity. Also, a tilt error on the accelerometer platform leads to errors in the correction for gravitation, resulting in horizontal acceleration errors. Both the velocity drift and tilt problem are, however, slowly varying. It has been found that if the autofocus is performed after the "raw" INU mocomp has been applied, autofocus on one single subwindow suffices to focus an entire strip.

V. System Calibration

Calibration is an important issue in modern remote sensing radars, and thus the EMI SAR are designed to facilitate system calibration. The stability of the system was ensured by applying design techniques usually applied in radiometer systems; e.g., all analog components,

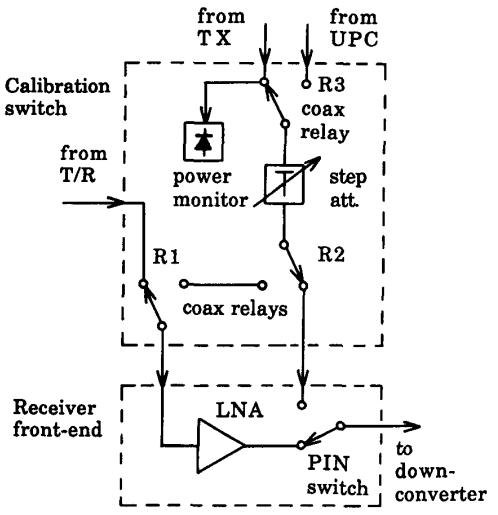

Fig. 6. Calibration switch.

including the TWT, are temperature stabilized to 40°C ± 1°C. Careful measurements of the type described in [13] on the combined receiver and up-converter (excluding the transmitter) have shown an amplitude stability of ±0.10 dB and a phase stability of ±0.14° over this temperature range for several hours. Another important feature of radiometers is frequent automatic calibration. The KRAS radar has a number of internal calibration loops. Samples of the driver signal and TWT high-power output (sampled via a −50 dB coupler) are injected into the calibration switch (see Fig. 6). The calibration switch includes a pulse peak power monitor, an integrated pulse energy detector, and a programmable precision attenuator. The drive signal or the attenuated high-power output can be injected into the receiver either before or after the low-noise amplifier. In general, coax relays are used due to their low loss and high isolation properties, but after the LNA, a fast (100 ns) PIN switch enables switching from the calibration mode to the reception mode between pulse transmission and echo reception (and vice versa). The system thus holds the capability of routing each transmitted pulse through the calibration switch and the complete receiver chain for digitization and recording along with the received echo signal. This mode, however, requires that a significant portion of the record window be used for calibration; e.g., 2048 out of 8192 range cells when 20-μs pulses are transmitted in the high-resolution mode. The standard operation is therefore to record samples of the transmitted pulse just before each mapping track. The calibration loop, including the TWT, has an accuracy of 0.2 dB, and stability measurements have shown that this level of accuracy persists for hours after the calibration.

It is recognized that calibration requires characterization of the antenna and radome. A significant uncertainty in backscatter measurements can be attributed to insufficient knowledge of the antenna pattern. Accurate measurements of the SAR antenna were therefore undertaken in the spherical near-field antenna measurement facility of the Electromagnetics Institute, which has a measurement accuracy of better than 0.1 dB. During the measurements, the antenna was installed in the 4.6-m-long pod and the radome was mounted. The measurements showed that the mainbeam changed less than 0.1 dB as a function of the pointing angles set by the motion-compensation system. Based on these measurements, the effect of multipath propagation due to reflections from the wings are expected to be negligible, which is supported by the fact that it has not been possible to detect interference fringes in the data recorded so far.

A major calibration uncertainty in the system is due to errors in the antenna pointing. The errors can be separated into errors due to limited accuracy of the INU attitude measurement, and errors caused by the antenna-pointing system. Azimuth errors are of minor concern, since the antenna pointing is easily estimated by Doppler tracking. Elevation pointing errors are, however, not easily corrected, and especially at the edges of the swath, far away from the antenna boresight, the radiation pattern changes rapidly with angle. The pointing error due to the antenna gimbal is limited to 0.2°, and the INU attitude uncertainty contributes 0.1°. At steep incidence angles an important contribution comes from uncertainty in the altitude determination. As previously mentioned, a 50-m altitude error will give a 0.6° incidence-angle for a 12-km altitude and 20° incidence angle. At the edges of the mainlobe the two-way gain error amounts to approximately 1 dB per degree.

The processor calibration is presently in progress. Once measured, the antenna pattern in the azimuth direction is easily taken into account in the calibration of the processor. The Doppler tracker ensures that the processed part of the Doppler spectrum has been received from the azimuth direction with maximum antenna gain. If STC is applied, it is neutralized in the data processor before range compression, thereby avoiding distortion of the dispersed pulse. Radiometric corrections for the antenna elevation pattern and range attenuation are applied after the range compression.

Despite the potential system stability of 1 dB including sensor, pointing, and processor contributions, the system calibration will be supplemented with external measurements using corner reflectors. For operational mapping missions it is planned to map the corner reflectors deployed at and near the Technical University before and after the flights.

VI. Data Processor

During mapping, the data from the digital preprocessor are recorded on high-density digital tapes (HDDT). Subsequently, data are processed in the laboratory on an Apollo DN 10000 (extended RISC) equipped with 16 megabyte of main memory, one 330 megabyte system disk and two 660 megabyte data disks. Data are transferred from the HDDT to the Apollo via an IEEE 488 bus.

The SAR processing software is based on the range-Doppler algorithm, which corrects for the range curvature by interpolating range shifts in the range-doppler domain [14]. The performance of the FFT transform plays an important role in this algorithm, and potential advantages of using alternative fast transform or convolution algorithms were therefore studied [15]. The FFT was selected as the most suitable, primarily because some of its alternatives call for special-purpose hardware.

The first version of the off-line processor was intended to support the radar development and design of the real-time processor. Accordingly, flexibility was the primary concern, not processing speed. This processor has now been upgraded to one that is more operationally suitable with a better human interface. Without sacrificing much of the flexibility, a somewhat faster version has been developed.

The processor is divided into three processing modules. The range module operates on data in range-sequential order. It offers one or more of the options: Doppler centroid estimation, first-order motion compensation, azimuth prefiltering, range walk correction, range compression, second-order motion compensation, and unfocussed SAR processing. The sequence of these options can be selected as desired. The output from the range module is typically (but not necessarily) scaled, converted to 16-b I and 16-b Q and stored on disk. Following the corner turning module, the azimuth module offers azimuth compression (including range-curvature correction), slant-to-ground-range resampling, detection, multilooking, and intensity transformation.

The processor also holds an analysis module, including histogram analyzer, spectrum analyzer, Doppler rate estimator (autofocus module), and INU data analyzer.

The off-line processor takes about 3 h to process a 9 by 6 km image into 2-m resolution. Recently, the disk organization has been changed so that 9 by 24 km scenes can be processed, and using the airborne real-time azimuth prefilter, the maximum scene size is 9 by 48 km at 2-m resolution, or 36 by 48 km at 8-m resolution.

VII. Performance Evaluation

In November and December 1989 the first flight tests of the Danish airborne SAR were performed. The first flight demonstrated that the system generated quality imagery, albeit at a reduced resolution (8 by 8 m) due to a sampling rate error and lack of INU data. On the second mission, Copenhagen and the Technical University of Denmark were mapped with a resolution of 2 by 2 m (see Fig. 7). The data (which included the Technical University of Denmark and central Copenhagen) were acquired at an altitude of 41 000 ft ($\approx$ 12 500 m), a slant range of 22 000 to 31 200 m, transmitting an 80-MHz linear FM signal and using an antenna tilt-angle of 65°. Since no STC was applied, it is seen from Fig. 3 that the power returned for a constant σ° will vary approximately 1.5 dB from near-range to far-range, which is supported by the fact that the processed images are very well balanced radiometrically. The equalization of the radiometric response across the swath is entirely due to the antenna shaping, combined with the appropriate scaling of reference functions in the SAR correlator, effectively keeping the noise gain constant. It is noted that there are no interference fringes indicating reflections from the wing, and there is no "banding" effect in the along-track direction indicating motion-compensation problems.

A. Resolution

By using three-corner reflectors located on a soccer field at the University (Fig. 7(b) and 8), a resolution of 2.0 $\pm$ 0.02 m in range and 2.1 $\pm$ 0.04 m in azimuth was measured, showing that the 2 by 2 m design goal for the resolution has been met.

B. Sidelobes

The peak sidelobes were measured to be -22 ± 1 dB in range and -20.5 ± 1 dB in azimuth, which is to be compared with the theoretical value of -22 dB for the applied filter weighting. Considering that the clutter was only 30 dB below the corner reflector peaks, a better correspondence is not to be expected.

In 1990 the tests were continued. The testing has included operating the system in all of the three mapping configurations shown in Fig. 1; i.e., the ERS-1 underflight configuration and the 80-km range fine and course-resolution configurations. The latter involved testing the real-time range filters. The real-time Doppler tracker, Mocomp 1, and the azimuth prefilter have been tested also. Finally, the "automap" control software assisting the SAR operator has been tested.

VIII. Present Activities and Future Plans

The system test and verification is an on-going activity, with focus especially on the system calibration. The processor calibration is in progress and the absolute calibration accuracy of the system is still to be measured.

In parallel with the above activities, the development of a real-time on-board processor and display system is being undertaken. This processor will have the capability of producing single-look imagery from one SAR channel, full swath and full resolution real-time in-flight. It is expected that the real-time processor will be available by early 1992.

Funding has been approved for developing a prototype of a dual-polarized microstrip antenna, and it is anticipated that this work will lead to an update of the system to full polarimetric capability.

The primary objective of the presented work is research in coherent radar technology and data processing algorithms, but the scientific utilization of the SAR is an obvious extension. The European Space Agency's ERS-1 *C*-band satellite is expected to be launched in 1991 and this will lead to a major increase in SAR-related activities in Europe. Also, the Joint Research Center, of the Euro-

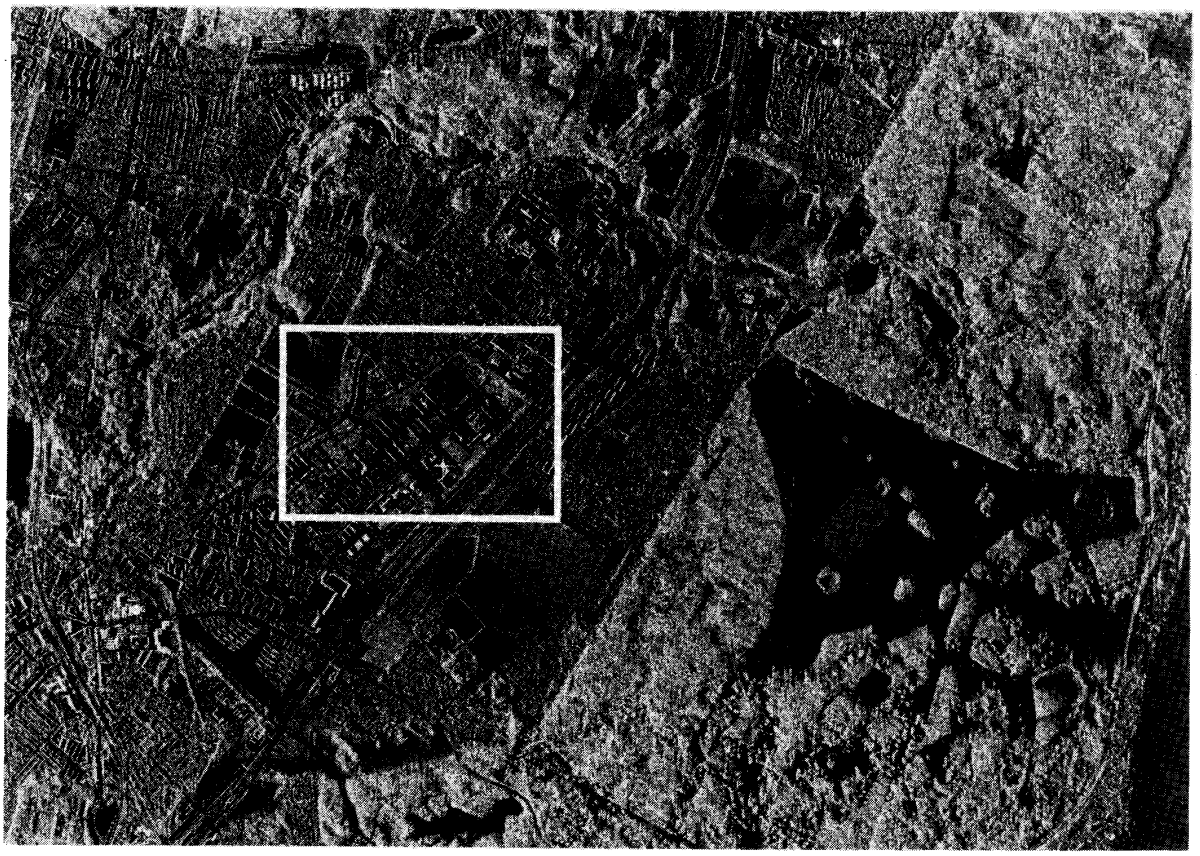

(a)

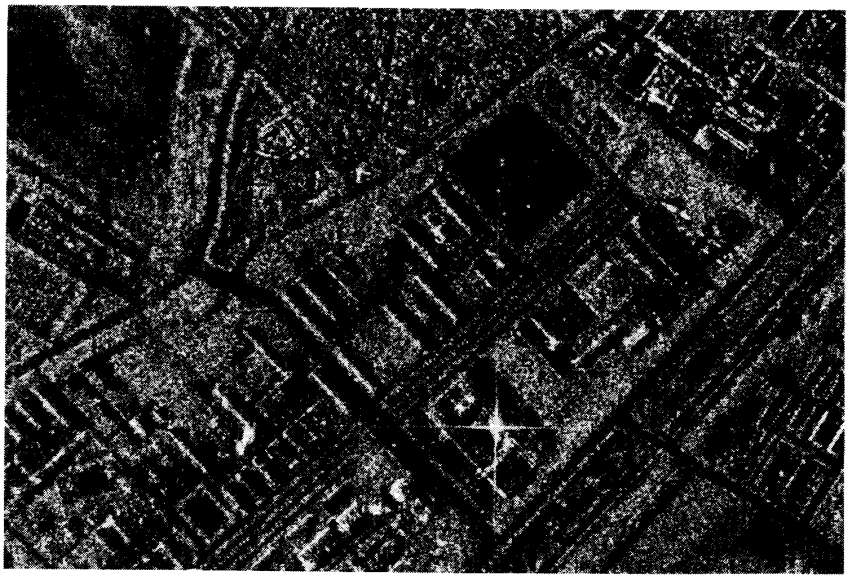

(b)

Fig. 7. (a) The Technical University of Denmark mapped on December 6, 1989, in the Danish SAR's second test flight. (b) Subwindow showing the soccer field (right above center) where the three corner reflectors are located.

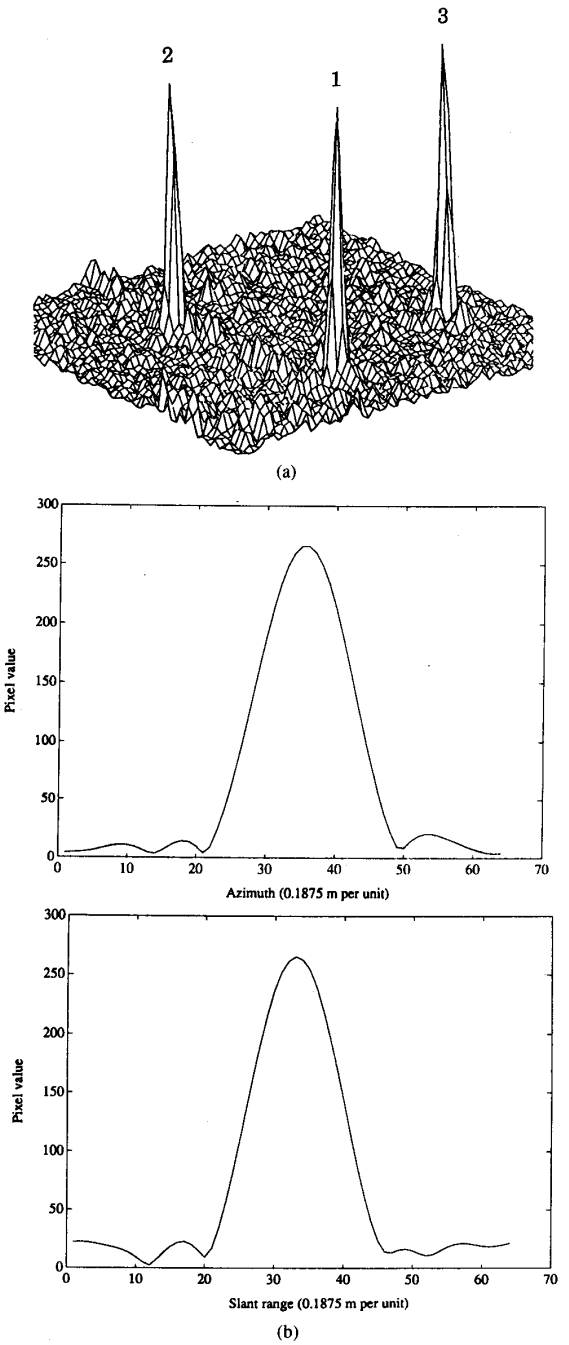

Fig. 8. (a) Three-dimensional plot of the response of corner reflectors on the soccer field (linear amplitude scale). (b) Azimuth (top) and range (bottom) cuts through one corner reflector.

pean Economic Community, has decided to improve the possibilities for the acquisition of remote sensing data and to support the establishment of an operational source for airborne optical and microwave remote sensing measurements. As a result of this initiative the European Airborne Remote Sensing Facility (EARSEF EEIG) has been established. The Danish SAR is the main microwave sensor of EARSEF, in addition to being a testbed for radar research at the Technical University of Denmark. The goal of EARSEF is to have an operational SAR available in Europe on request, and such a system may emerge during the next few years.

Acknowledgment

The authors would like to acknowledge key members of the KRAS team: A. Netterstrøm and A. Østergaard (digital front end), K. Woelders (control computer), M. Dich (antenna), J. Hjelm Jørgensen and F. Nygreen (digital signal processing), J. Granholm (analog electronics), and S. S. Kristensen (processor upgrade), as well as the contributions and know-how from many other colleagues at the Electromagnetics Institute.

References

[1] J. J. Kovaly, *Synthetic Aperture Radar*. Reading, MA: Artech, 1976.
[2] G. Duchossois, "Overview and status of the ERS-1 programme," Eur. Space Agency, ESA SP-254, vol. 1, Aug. 1986.
[3] E. Lintz Christensen, S. Nørvang Madsen, and N. Skou, "Review of the Homodyne technique for coherent radar," presented at the IEEE Int. Radar Conf. RADAR'90, Arlington, VA, May 7-10, 1990.
[4] A. Netterstrøm, "Using digital pre-distortion to compensate for analog signal processing errors," presented at the IEEE Int. Radar Conf. RADAR'90, Arlington, VA, May 7-10, 1990.
[5] J. Granholm, "A/D converter module for high-resolution SAR," Electromagnetics Instit., Tech. Univ. Denmark, Lyngby, Sept. 1990.
[6] F. Nygreen, "Range and Azimuth filters for Synthetic Aperture Radar," Electromagnetics Instit., Tech. Univ. Denmark, Lyngby, Dec. 1990.
[7] S. N. Madsen, "Estimating the Doppler centroid of SAR data," *IEEE Trans. Aerosp. Electron. Syst.*, vol. 25, pp. 134-140, Mar. 1989.
[8] M. Dich, "Slotted waveguide array antenna for Synthetic Aperture Radar," Electromagnetics Instit., Tech. Univ. Denmark, Lyngby, Sept. 1990.
[9] S. N. Madsen, N. Skou, and E. Lintz Christensen, "A new *C*-band SAR for ERS-1 underflights," presented at the IEEE Int. Radar Conf. RADAR'90, Arlington, VA, May 7-10, 1990.
[10] C. Høg and J. H. Jørgensen, "INU interfacing and motion compensation calculation for the Danish *C*-band SAR," Electromagnetics Instit., Tech. Univ. Denmark, Lyngby, Dec. 1990.
[11] K. Woelders "KRAS radar control unit overview," Electromagnetics Instit., Tech. Univ. Denmark, Lyngby, Oct. 1990.
[12] T. A. Kennedy, "Strapdown inertial measurement units for motion compensation for Synthetic Aperture Radars," *IEEE AES Magazine*, pp. 32-35, Oct. 1988.
[13] N. Skou, S. N. Madsen, E. Lintz Christensen, A. Netterstrøm, and K. Woelders "The Danish *C*-band SAR, calibration accuracy and stability," presented at IGARSS'90, Washington, DC, May 20-24, 1990.
[14] C. Wu, K. Y. Liu, and M. Jin "Modeling and a correlation algorithm for spaceborne SAR signals," *IEEE Trans. Aerosp. Electron. Syst.*, vol. AES-18, pp. 563-574, Sept. 1982.
[15] J. Dall, "Fast convolution algorithms for SAR processing," in *Proc. Int. Conf. Radar* (Paris), 1989, pp. 226-231.

Søren Nørvang Madsen obtained the M.Sc.E.E. degree in 1982, and the Ph.D. degree in 1987.

In 1982 he joined the Electromagnetics Institute, Technical University of Denmark, where his work has included all aspects of Synthetic Aperture Radar, including development of pre-processors, analysis of basic properties of SAR images, postprocessing, and SAR systems design. Since 1987 he has been an Associate Professor at the Electromagnetics Institute, working primarily with digital signal processing and radar theory. From

1986 to 1989 he was Project Manager for the Danish Airborne SAR programme. Since January 1990 he has been on leave, working for NASA's Jet Propulsion Laboratory, Pasadena, CA.

Erik Lintz Christensen received the M.Sc.E.E. degree in 1966.

In 1968 he joined the Electromagnetics Institute, Technical University of Denmark, where he is now an Associate Professor. His work has covered many aspects of radars, radio communications, and high frequency and microwave electronics. This includes the design of 60 and 300 MHz radars for the recording of the thickness of the inland ice of Greenland and Antarctica, equipment for measuring amplitude and phase of the transfer function of a 50-km line-of-sight radio path at 15 GHz, and a system for measuring amplitude and phase of antenna near-field patterns. He is now Project Manager of the Danish Airborne SAR programme.

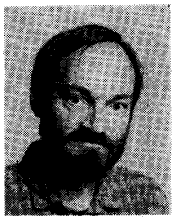

Niels Skou earned the M.S.E.E. (1972) and Ph.D. (1981) degrees at the Technical University of Denmark.

Presently, he is a Senior Research Associate at the Electromagnetics Institute of the University of Denmark. His research has been directed towards microwave remote sensing systems. After three years work with the development of radar systems for measuring the ice sheets in Greenland and Antarctica, his interest turned towards microwave radiometry. From 1975 to 1979 he developed the scanning multifrequency airborne radiometer system of the Electromagnetics Institute. Since then, his subjects have been radiometer measurements of sea ice and oil pollution on the sea, spaceborne radiometer systems, and the development of new systems for specific purposes. His interest has lately turned back to active instruments, and presently he is engaged in the development of the airborne *C*-band Synthetic Aperture Radar System.

Jørgen Dall received the M.Sc (1984) and Ph.D. (1989) degrees in electrical engineering from the Technical University of Denmark.

Since 1984 he has been with the Electromagnetics Institute at the Technical University of Denmark, where he is currently a Postdoctoral Fellow. His work has covered SAR processor development, SAR processing algorithms, fast transform and convolution algorithms, and VLSI architectures for digital signal processing. Also, he has been working with studies of imaging radars and altimeters for planetary missions. Currently, he is involved in the development of the Danish airborne SAR.